A Murari et al.

How to Assess the Efficiency of Synchronization Experiments in Tokamaks

How to Assess the Efficiency of Synchronization Experiments in Tokamaks

by A.Murari[1,2], T.Craciunescu[3], E.Peluso[4], M.Gelfusa[4], M.Lungaroni[4], L.Garzotti[5] D.Frigione[6] and P.Gaudio[4]and JET Contributors*

EUROfusion Consortium, JET, Culham Science Centre, Abingdon, OX14 3DB, UK

1) EUROfusion Programme Management Unit, ITER Physics Depratment, Culham Science Centre, Abingdon OX143DB

2) Consorzio RFX (CNR, ENEA, INFN, Universita' di Padova, Acciaierie Venete SpA),Corso Stati Uniti 4, 35127 Padova, Italy

3) National Institute for Laser, Plasma and Radiation Physics, Magurele-Bucharest, Romania

4) University of Rome "Tor Vergata", Via del Politecnico 1, 00133 Rome, Italy

5) CCFE, Culham Science Centre, Abingdon, Oxon, OX14 3DB, UK

6) Unità Tecnica Fusione - ENEA C. R. Frascati,via E. Fermi 45, 00044 Frascati (Roma), Italy

Abstract

Control of instabilities such as ELMs and sawteeth is considered an important ingredient in the development of reactor relevant scenarios. Various forms of ELM pacing have been tried in the past to influence their behaviour using external perturbations. One of the main issues of these synchronization experiments resides in the fact that ELMs are quasi periodic in nature and therefore, after any pulsed perturbation, if enough time is allowed to elapse, an ELM always occurs. To evaluate the effectiveness of ELM pacing techniques, it is therefore essential to determine an appropriate interval over which they can really have a triggering capability. In this paper, three independent statistical methods are described to address this issue: Granger Causality, Transfer Entropy and Recurrence Plots. The obtained results for JET with the ILW indicate that the proposed techniques agree very well and provide much better estimates than the traditional heuristic criteria reported in the literature. Moreover, their combined use allows improving the time resolution of the assessment and determining the efficiency of the pellet triggering in different phases of the same discharge. Therefore, the

developed methods can be used to provide a quantitative and statistically sound estimate of the triggering efficiency of ELM pacing in realistic experimental conditions.

1 ELM Pacing as synchronization experiments and causality

ELMs are instabilities that almost invariantly affect H mode plasmas, causing a reduction of the energy confinement through deterioration of the edge transport barrier [1]. This sudden degradation of the confinement at the edge induces an expulsion of energy and matter from the plasma on a sub millisecond time scale, which can result in unacceptable erosion of the plasma facing components in the divertor. Various statistical investigations of ELMs instabilities have reported contrasting results about their properties; some studies have detected a quasi-periodic behaviour, some a chaotic one and recently evidence of quasi chaotic ELMs has also emerged [2,3]. Irrespective of their dynamic nature, in the perspective of ITER and DEMO it is imperative to control ELMs carefully, to alleviate their detrimental effects on the plasma facing components in the divertor. Indeed, DEMO will probably have to be operated in ELM-free scenarios. On ITER, some form active ELM control is also considered essential. Therefore, to support the development of reactor relevant scenarios, in many machines various forms of ELM pacing techniques have been tested. This subject assumes a particular relevant role in the present programme of JET with an ITER Like Wall (ILW) on the route to the next full DT campaign [4].One of the most promising applications is pacing of ELMs with pellets [5,6]. The long term aim of this approach would consist of being able to trigger ELMs with pellets, whose frequency could be adjusted so that the gradients at the edge would not increase, between two subsequent ELMs, to the point of causing excessive expulsion of energy and matter, capable of damaging the plasma facing components. These pacing experiments are typical cases of synchronization techniques.

One of the main difficulties in developing such experimental solutions reside in the interpretation of the experimental results. This is due to the fact that ELMs are quasi periodic in nature and therefore, after any sudden perturbation such a pellet, if enough time is allowed to elapse, an ELM always occurs. To evaluate the effectiveness of the triggering, it is therefore essential to determine a reasonable time over which pellets can really have a triggering capability. This is equivalent to determining the time interval over which pellets can have a causal influence on the ELM dynamics. The difficulty of the problem can be appreciated by inspection of Figure 1, which reports the D_α for ELMs and pellets in a JET discharge with the ITER Like Wall (ILW). It is evident how the task of determining how

many pellets have triggered an ELM is quite challenging, given the limited diagnostic information and the high level of noise in the measurements. This is the typical problem of assessing causality relations between different events in a probabilistic framework.

Unfortunately even in science, there is no unique definition of causality and therefore it is impossible to identify a single, unique measure of cause-effect relationships. On the other hand, even if originally conceived to explain strong regularities in nature, causality relationships are often investigated in the framework of uncertainty. Moreover, again given the uncertainty implicit in many phenomena, it is important to be able to quantify also the strength of the causal relationships. Therefore, a probabilistic and not only a deterministic account of cause-and-effect relations is appropriate in the case of scientific problems affected by uncertainty. These considerations are particularly relevant to ELM pacing, given the complexity of the experiments, the strongly nonlinear character of these instabilities and the high level of noise and uncertainties in the measurements. A statistical analysis becomes
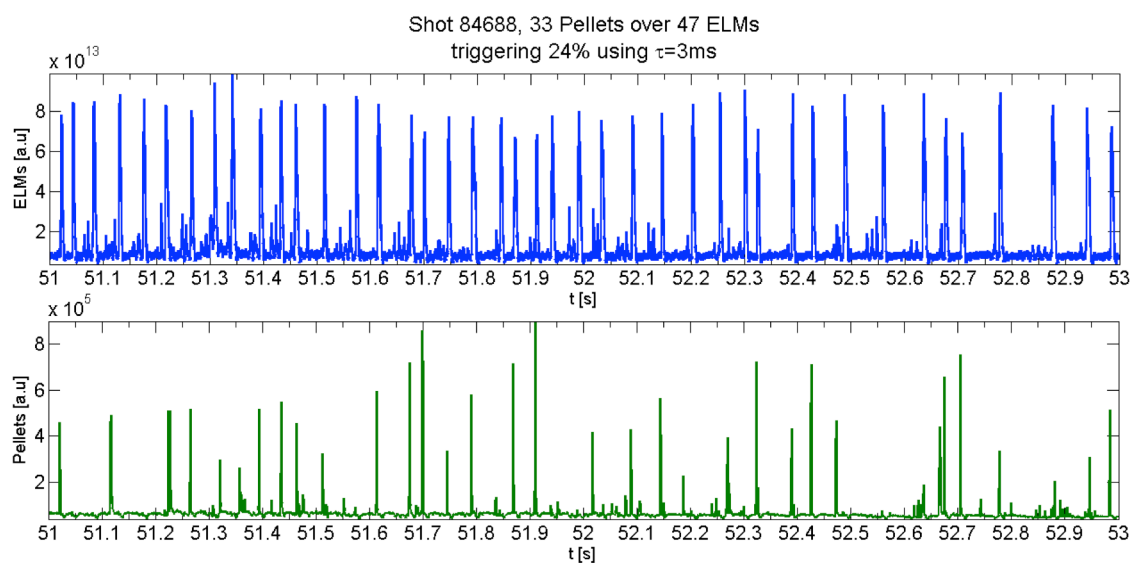
Figure 1. Top: Dα signals identifying the occurrence of ELMs Bottom: Dα signal indicating the arrival of the pellets into the plasma.

therefore indispensable to complement more traditional dynamical studies.

In this work, three statistical criteria to determine causality between external perturbations and ELMs are introduced. The first two are purely statistical approaches to the determination of causality. They are based on the definition of causality introduced by Wiener [7], which, even if very vague, was the first one susceptible of being computationally measured. The main idea is that, given two measurements, if it is possible to better predict the

first given the knowledge of the past of the second, then the second can be considered causal to the first. This restricted sense of causality, based on predictability, was adopted by Granger, who proposed a practical way of calculating it [8]. This *Granger Causality* (GC) has been deployed successfully in many fields, ranging from economics to climatology and the neurosciences. This is the first method which, properly adapted, has been applied to the problem of assessing the efficiency of ELM pacing on JET. On the other hand, Granger Causality was traditionally measured assuming a linear regression model, which is not fully general. In the case of strongly nonlinear systems, therefore, the conclusions of the traditional Granger Causality could be questioned. The same definition of causality, as incremental predictability, has therefore been implemented also using a non-parametric, nonlinear indicator, called Transfer Entropy [9]. Transfer Entropy (TE) is an information theoretic functional of probability distribution functions and measures the exchange of information between signals. TE has been explicitly conceived to analyse time series and investigate their causal relationship on the basis of predictability and information transfer.

The third method developed is more typical of nonlinear dynamical studies and it is based on Recurrence Plots. Indeed, the recurrence behaviour is a fundamental characteristic of dynamical systems. Recurrence plots are very powerful tools for the descriptive studies of the statistical properties of dynamical systems [10]. A recurrence plot (RP) is a plot showing the times at which a phase space trajectory visits roughly the same area in phase space. Joint Recurrence Plots (JRP) can be used to relate the behaviour of one signal with the one of another. By quantifying the properties of JRP through Recurrence Quantification Analysis (RQA), it is possible to determine the maximum interval of information transfer between two time series [10]. As shown later, this proves to be a very good estimate of the interval over which a system exerts a causal influence on another.

It is worth emphasizing that, in this paper, the term causality is used only in the restricted sense of improved predictability and information transfer between time series, without any reference to the philosophical implications of the word. Given the nature of the application presented, this is not a relevant issue because it is known a priori that pellets can trigger ELMs and not vice versa; therefore philosophical discussions about root and real causes are not relevant.

With regard to the structure of the paper, the next sections provide the mathematical background to the main criteria used in the paper: Granger causality is explained in Section 2, Transfer Entropy is introduced in Section 3 and the background on Recurrence Plots is provided in Section 4. Some numerical tests with synthetic data are reported in Section 5, to

illustrate the potential of the proposed techniques to identify the interval of cause-effect relations in time series of the type encountered in practice. The proposed indicators are then applied to ELM pacing with pellet in Section 6,using data of JET discharges with the ITER Like Wall (ILW). Conclusions and discussion of possible future developments of the proposed techniques are the subject of the last Section of the paper.

2 Granger Causality: approach and mathematical background

Granger causality is a form of "predictive causality" in the sense that causal relations are measured by determining the ability to predict the future values of a time series using prior values of another time series. A time series J is said to Granger-cause I if it can be shown, through an appropriate series of statistical tests on lagged values of J, that those J values provide significant information about future values of I.

Granger causality is therefore based on two principles:

1. The cause happens prior to its effect.
2. The cause has *unique* information about the future values of its effect.

Starting from these two assumptions about causality, the identification of a causal effect of J on I is performed in the context of linear regression models with the procedure described in the following. The analysis is typically formulated as a hypothesis testing problem. Given two stationary time series I and J, to test the null hypothesis that J does not Granger-cause I, one first finds the proper lagged values of I to include in a univariate auto regression model of I:

$$I(t) = a_0 + a_1 I_{t-1} + a_2 I_{t-2} + ... + a_m I_{t-m} + \eta_1(t) \quad (1)$$

where $\eta_1(t)$ indicates the residuals. Next, the auto regression model is augmented by including lagged values of J:

$$I_J(t) = b_0 + a_1 I_t ...... + a_m I_{t-m} + b_1 J_t ...... + b_m J_{t-m} + \eta_2(t) \quad (2)$$

In the traditional Granger-Sargent test, the coefficients are estimated via the ordinary least-squares technique. The model order m can be selected using model selection methods such as the Akaike of the Schwarz criteria [11].

The prediction improvement PI_{J-I} can be defined as a function of the minimized residuals:

$$PI_{J-I} = S_{\eta 1}(t) - S_{\eta 2}(t) \qquad (3)$$

where S indicates the variance of the residuals. The higher the value of this indicator the better is the prediction of I when the signal J is taken into account. Therefore the higher the value of PI_{J-I} the more information J carry about I and therefore the more causal J can be considered to I. In practice, of course, the estimator can take positive values due to random fluctuations. Therefore a criterion is needed to decide whether an influence of J on I is really present at a certain confidence level. It can be demonstrated that the quantity

$$F_{J-I} = \quad (N-3m-1)[S_{\eta 1} - S_{\eta 2}]/mS_{\eta 2} \qquad (4)$$

is distributed according to the Fisher's F-law with (m,N-3m-1) degrees of freedom (N is the total number of available points in the time series) [15]. Therefore, it can be stated that causal influence of J on I exists at the significance level p if the value of F_{J-I} exceeds the (1-p) quantile of the respective F distribution. This means that if F_{J-I} exceeds the (1-p) quantile of the respective F distribution, the probability of random error in detecting causality is less than p. To obtain the results shown in this paper, the GC has been calculate using the consolidated spectral method reported in [8].

GC can be used basically in two different ways. In the case of various time series, whose relationship is not known, GC can help determining their causal dependencies. In the case the cause-effect relation between two signals is already known, GC can help assessing the length in time over which this relation lasts; the most direct approach consists of determining the longest interval over which F_{J-I} exceeds the (1-p) quantile of the F distribution, i.e. the longest interval over which the null hypothesis is not valid, at the selected significance level.

3 Transfer Entropy: concept and mathematical background

In this Section, the basic mathematical and information theoretic background of Transfer Entropy is introduced. A good entry point to understand Transfer Entropy is the Kullback Entropy (KE). The KE is defined as:

$$K_I = \sum_i p(i)\log\left(p(i)/q(i)\right) \quad (5)$$

Where p and q are two probability density functions (pdfs). The Kullback Entropy assumes always positive values and is zero only when the two pdfs, p and q, are exactly the same. Therefore the smaller the KE is, the closer the pdf $q(i)$ is to the reference one $p(i)$. So KE can also be thought as the error committed by approximating pdf p with pdf q. In information theoretical terms, the KE can be interpreted as the excess number of bits that have to be coded if a different pdf $q(i)$ is used instead of $p(i)$.

The KE can also be expressed in terms of conditional probabilities p (i | j):

$$K_J = \sum_i p(i|j)\log\left(p(i|j)/q(i|j)\right) \quad (6)$$

It is also possible to express KE in terms of joint probabilities, whhc allow sintridcing the mutual information M_{IJ} between two processes I and J. The mutual information can also be interpreted as the excess of code required if one assumes erroneously that the two systems are independent. The M_{IJ} can be defined as:

$$M_{IJ} = \sum_i p(i,j)\log\left(\frac{p(i,j)}{p(i)p(j)}\right) \quad (7)$$

Where the reference is the case of independent events (the two pdfs are factorised at the denominator of the logarithm). Again, complementary to the interpretation in terms of additional code required, the M_{IJ} can also be considered the error committed by considering independent pdfs which are not.

Unfortunately, the mutual information is a symmetric quantity and therefore cannot provide any information about directionality. On the other hand, M_{IJ} can be given a direction by introducing a time lag τ between the processes:

$$M_{IJ}(\tau) = \sum_n p(i_n, j_{n-\tau}) \log \left(\frac{p(i_n, i_{n-\tau})}{p(i)p(j)} \right) \quad (8)$$

This last step suggests that, in order to obtain information about the dynamical structure of the processes to be investigated, one can reformulate the previous quantities in terms of transition probabilities instead of static probabilities. To this end, the formalism of Markov processes is the most natural and useful to adopt. For words of length k, using the synthetic notation $i_n^{(k)} = (i_n, \dots, i_{n-k+1})$, the following relation is satisfied by a Markov process of order k:

$$p(i_{n+1}|i_n, \dots, i_{n-k+1}) = p(i_{n+1}|i_n, \dots, i_{n-k}) \quad (9)$$

At this point, one important quantity to remember is the entropy rate h_I, which quantifies the number of bits needed to encode one additional state of the system if all previous ones are known. The definition of the entropy rate is:

$$h_I = -\sum p\left(i_{n+1}|i_n^{(k)}\right) \log\left(i_{n+1}|i_n^{(k)}\right) \quad (10)$$

The entropy rate is the most fruitful quantity to extend to two processes for the study of causal relationships. This can be achieved by measuring the deviation from the generalised Markov property:

$$p\left(i_{n+1}|i_n^{(k)}\right) = p\left(i_{n+1}|i_n^{(k)}, j_n^{(l)}\right) \quad (11)$$

The main idea behind relation (11) is that, if there is no flow of information from J to I, the state of J should have no influence on the transition probabilities of I. The level of inadequacy of this assumption can be quantified with a generalization of the Kullback Entropy, called the Transfer Entropy (TE) and defined as:

$$T_{J \to I} = \sum p\left(i_{n+1}, i_n^{(k)}, j_n^{(l)}\right) \log \left(\frac{p\left(i_{n+1}|i_n^{(k)}, j_n^{(l)}\right)}{p\left(i_{n+1}|i_n^{(l)}\right)} \right) \quad (12)$$

In the case the cause-effect relation between two signals is already known, as in the application described in this paper, TE can help determining the length in time over which this relation lasts; this can be achieved by scanning parameters l and k in equation (12). A full mathematical derivation of the TE is provided in [9] and the references therein.

4 Recurrence Plots

As mentioned already, the recurrence behaviour is a fundamental characteristic of dynamical systems. Recurrence plots are very powerful tools for the descriptive studies of the statistical properties of complex and chaotic systems. A recurrence plot (RP) is a plot showing the times at which a phase space trajectory visits roughly the same area in the phase space. In more detail, the recurrence plots depict the collection of pairs of times at which the trajectory returns sufficiently close the same place. RPs are based on the following matrix representation:

$$R_{ij} = \Theta\left(\varepsilon - \left\|\vec{x_i} - \vec{x_j}\right\|\right), \quad i,j=1,\dots,N \tag{13}$$

where: $\vec{x_i}$ stands for the point in phase space at which the system is situated at time i, and ε is a predefined threshold. As $\Theta(x)$ is the Heaviside function, the matrix consists of the values 1 and 0 only. The graphical representation is an $N \times N$ grid of points, which are encoded as black for 1 and white for 0.
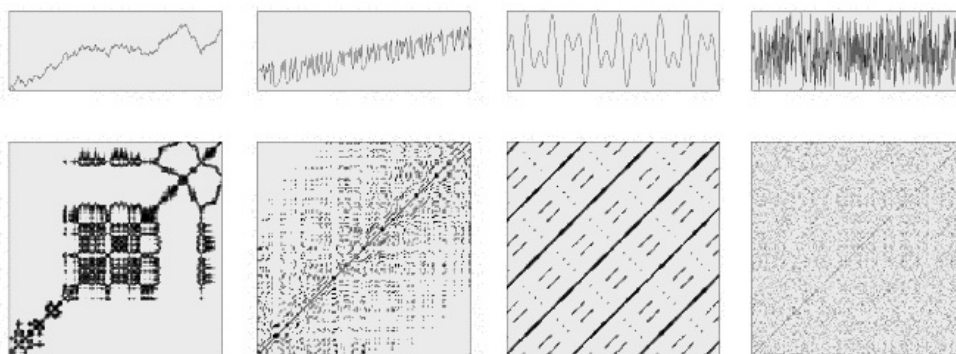

Figure 2 – Examples of typical recurrence plots. In the top row examples of time series are plotted versus time; in the bottom row the corresponding recurrence plots are shown. From left to right: data from an auto-regressive process, chaotic data with linear trend (logistic map), harmonic oscillation with two frequencies and uncorrelated stochastic data (white noise).

A black point in the RP means that the system returns to an ε-neighborhood of the corresponding point in phase space. This recurrence gives the name to the method. A number of examples, for different types of dynamical systems, are reported in Figure 2.

Multivariate extensions of recurrence plots have been developed. The most relevant for the applications described in this paper are the joint recurrence plots (JRP). Joint recurrence plots are the Hadamard product of the recurrence plots of the considered sub-systems (Romano et al. 2004), e.g. for two systems x and y the joint recurrence plot is:

$$\mathbf{JR}(i,j) = \Theta(\varepsilon_x - \|\mathbf{x}(i) - \mathbf{x}(i)\|)\, \Theta(\varepsilon_y - \|\mathbf{y}(j) - \mathbf{y}(j)\|) \quad \mathbf{x}(i) \epsilon R^m, \mathbf{y}(j) \epsilon \ R^n \ i,j= ,\ldots\ldots.N_{x,y} \ (14)$$

In contrast to cross recurrence plots, joint recurrence plots compare the simultaneous occurrence of recurrences in two (or more) systems. Joint recurrence plots can be used to detect phase synchronisation.

In addition to allowing an easy visualization of the periodicities of dynamical systems, RPs and JPRs permit to quantify very important properties of a system phase space: this is the so called recurrence quantification analysis (RQA). RQA is based on the distributions of the diagonal, horizontal and vertical lines that are found in the RP. The synergy between RPs and RQA forms a powerful tool and both methods have been widely applied in many fields such as physics, medicine, earth sciences and economics.

Of particular relevance for the subject of this paper is the fact that RQA provides several measures, which can be related to the causal relation between signals:

- Average Diagonal Length: The averaged diagonal line length can be calculated as

$$L = \frac{\sum_{\ell=\ell_{\min}}^{N} \ell\, P(\ell)}{\sum_{\ell=\ell_{\min}}^{N} P(\ell)} \qquad (15)$$

Where $P(l)$ is the frequency distribution of the lengths l of the diagonal lines. This indicator is related with the *predictability time* of the dynamical system.

The *determinism (predictability)* is a measure based on diagonal lines:

$$DET = \frac{\sum_{l=l_{min}}^{N} lP(l)}{\sum_{l=1}^{N} P(l)} \qquad (16)$$

DET is based on the distribution of the lengths of the diagonal lines $P(l)$ of length l that are found in the plot. Processes with uncorrelated or weakly correlated, stochastic or chaotic behaviour present none or very short diagonals, whereas deterministic processes show longer diagonals and less single, isolated recurrence points. Therefore DET is a measure of the determinism (predictability) of the system. The threshold l_{min} excludes the diagonal lines which are formed by the tangential motion of the phase space trajectory. The great interest of the diagonal lines, and implicitly of DET, derives from the fact that they are linked to the largest Lyapunov exponent if there is an underlying dynamical system. The length of the lines is related to the inverse of the largest positive Lyapunov exponent [10]. *DET* can be interpreted also as the probability that two closely evolving segments of the phase space trajectory will remain close for the next time step.

JRPs and in particular the parameters which can be derived using RQA can be used to determine the causality horizon, the longest time interval over which it is reasonable to assume that a system influences another. Indeed, various parameters obtainable with RQA show a clear maximum for the appropriate lag time corresponding to the causality horizon. This is the criterion adopted to derive the result reported in the rest of the paper.

5 Results of numerical test with synthetic data

The three proposed methods have been extensively tested with synthetic data to prove their capability to identify causal relationships. In particular, it has been verified that they can properly determine the right interval over which signal *J* exerts a causal influence on signal *I*. In this Section, some numerical examples are reported to show how the proposed methods can be applied directly to time sequences affected by noise. The effect on sequence I of sequence J, containing signal components causing I, is quantified. The first numerical example involves more traditional and smooth signals. The second example is meant to prove

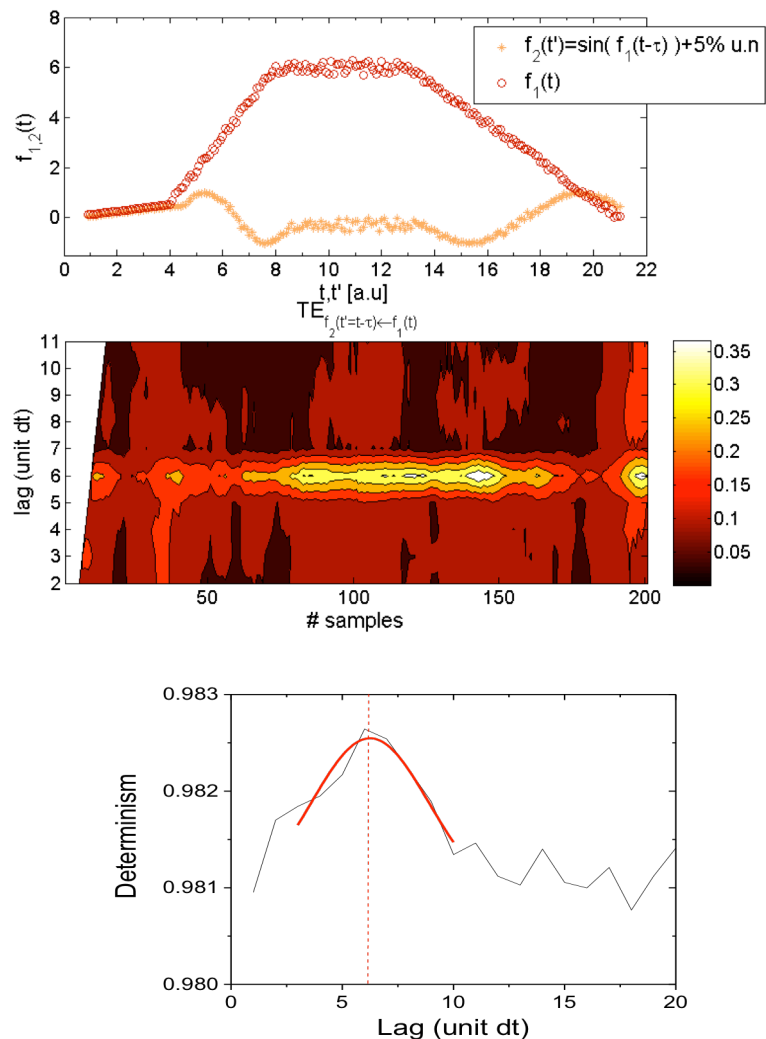the capability of the three techniques to handle also spiky signals, of the type characteristic of ELMs.

Figure 3. Top, synthetic signals; Middle, TE showing a clear maximum at $\tau = 6dt$; Bottom, determinism shows also a maximum at $\tau = 6dt$.

The first test has been performed computing twenty one time sequences of functions having a trapezoidal shape; then each synthetic signal has been used as the argument of a sinusoidal function with a delay of $\tau = 6dt$ (see Figure 3). Finally a random 5% uniform noise has been added on each couple of time sequences and the TE computed. GC identifies the right lag time of 6dt at 5% significance level. Figure 3 shows the functions and the TE results, where the brighter the colour the higher the transfer entropy. It is evident that the delay has been detected correctly. The JRPs also show a clear distinctive peak at the right time lag, as reported also in Figure 3 for the determinism.
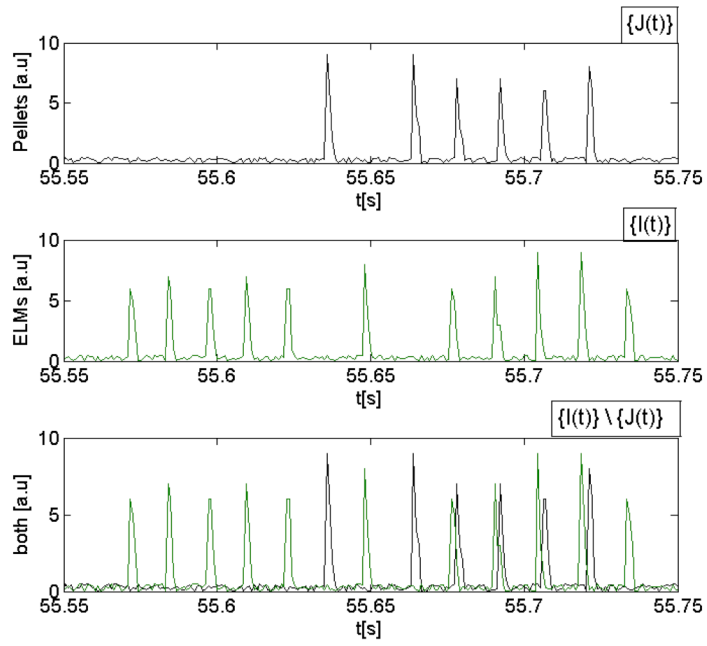
Figure 4.Top, signal J simulating pellet signals, middle I\J, simulating natural ELMs synthetic ELMs. Bottom, both signals.
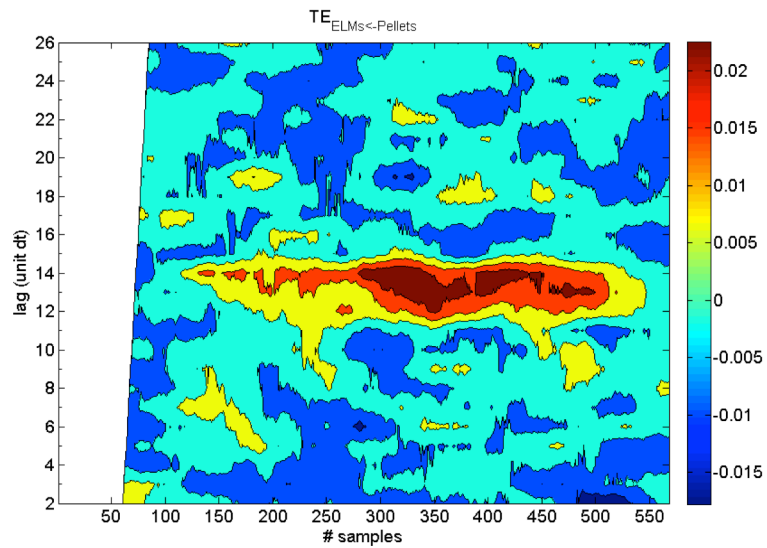

Figure 5.The higher the TE, the redder the colour. On the abscissa the number of samples, on the ordinate the lag between signals.

As mentioned earlier, a second specific example is reported to verify the applicability of the methods to spiky signals. Since, in the analysis of real experiments, the three techniques will be applied to signals related to instabilities, which can present quite abrupt variations, it has been double-checked that the three techniques can properly function even with this typology of data. Indeed in the literature there are no many applications of the introduced techniques to this type of signals; therefore numerical tests to verify their effectiveness also in this case are necessary. An example of the signals used for the systematic tests performed with synthetic data is reported in Figure 4. A series of triangularly shaped pulses, each with different slope and height, has been generated first, simulating the I signal (red triangles in Figure 4). Then a lower number of triangularly shaped pulses has also been generated, to simulate the signal J (blue triangle in Figure 4). Then, for each spike in the J signal, a corresponding spike on I has been generated after a temporal lag of $\tau = 15dt$. Finally, a random uniform noise has been added. To improve the readability of Figure 4, the amplitude of each peak is one thousand times the noise, but the same results have been obtained using a signal to noise ratio of ten. The test reported has been performed using twenty couples of time sequences each having a different time length.

The GC identifies the right mean time lag at 5% significance level, adopting the usual criterion of choosing as lag time the longest interval for which the null hypothesis is falsified. With the Transfer Entropy, the estimate has been obtained computing the mean of TE for each lag unit among all the couples and then considering the maximum obtained. The results indicate clearly that the ratio $\frac{TE_{J \rightarrow I}}{TE_{I \rightarrow J}} \sim 2.5$ and that TE has a maximum at τ=15dt, confirming
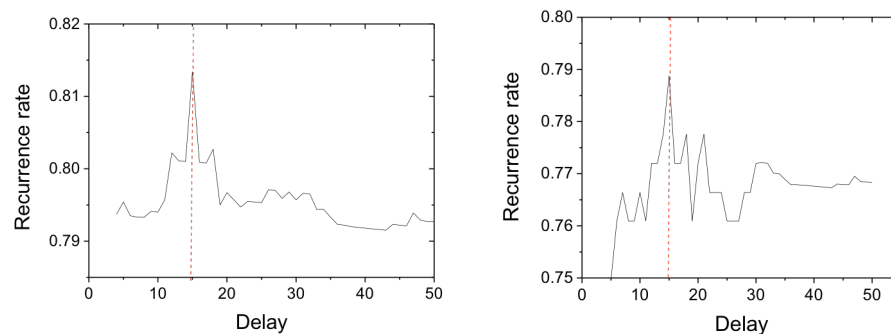

Figure 6. Recurrence rate: left no noise, right 5% noise signals.

that TE can identify both the real causal relationship and the right lag time also for this type of signals. The identified lag time versus the number of samples is reported in Figure 5.

The recurrence plots manage also to properly identify the correct lag time. Moreover, various indicators obtained with RQA provide the same estimate. In Figures 6 and 7 the
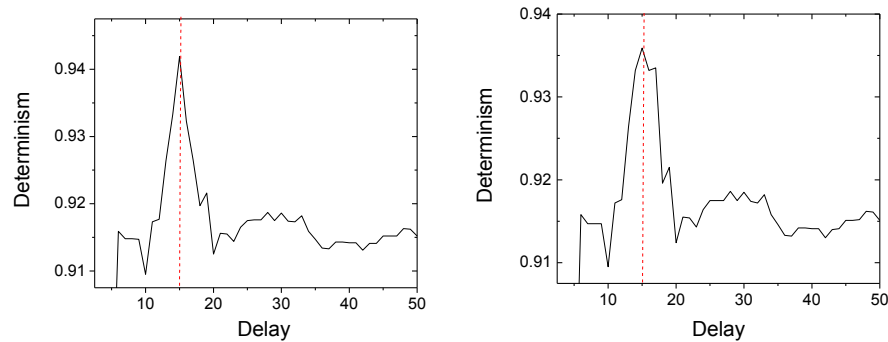

Figure 7 Determinism. Left without noise, right with 5 % additive noise.

Recurrence Rate and determinism are plotted versus the lag time. The recurrence rate is the percentage of recurrence points in a JRP and corresponds to the correlation sum. Determinism is the ratio of recurrence points that form diagonals structures to all recurrence points. If the systems have similar phase space behaviour the amount of longer diagonals increases. Both indicators exhibit a clear peak for the correct delay of 15 time units, for both the case with and without noise.

It is worth mentioning that, since the pulses have a finite width, the results cannot be provided with a resolution higher than plus minus a lag time. A numerical study has been performed also to investigate the effect of the finite size and the noise in the experimental measurements.

6 Application to ELM pacing with pellets

As mentioned earlier, one of the main issues with the interpretation of pellet pacing experiments is the evaluation of which ELMs have indeed been triggered by pellets. On JET, from basic physical reasons, it has always been assumed that a pellet can trigger an ELM only if the time between the two events is less or equal to 2 ms. In order to test this working hypothesis, the three techniques introduced in the previous sections have been applied to a set of 8 JET pulses, devoted explicitly to pellet pacing: 82885, 82886, 82887, 82889, 84688, 84690, 84693, 84696. The analysis has been performed using the D_α emission to determine

both the occurrence of the ELMs and the arrival time of the pellets in the plasma [5,6].For these discharges, sufficient statistics and signals of adequate quality are available to allow robust estimates. In particular these plasmas are sufficiently stationary, an implicit assumption for the application of the proposed criteria. The issue of increasing the time resolution will be discussed in the next section. On the other hand, this series of shots is not to be considered representative of the average performance of JET pellet injector, since also upgrades in the system have been recently implemented.
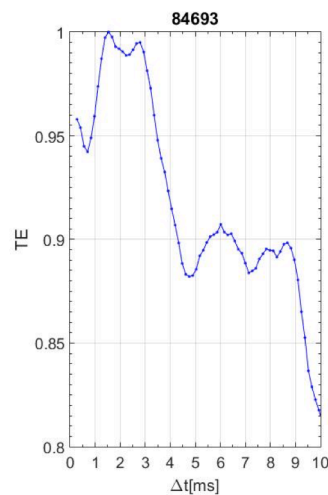

Figure 8.TE between pellets and ELMs for shot number 84693.

The main characteristics of the pellets injected in these discharges are reported in Table I. As can be seen from the Table, the parameter which has been varied over the widest range is the pellet speed.

To assess the time interval over which the pellets can be considered to have a triggering effect on the ELMs, the Granger Causality has been applied to the two time traces; the one of the ELM and the one of the pellets entering the plasma. By changing the lag time, the last instant, in which the null hypothesis is not verified at the 5% significance level, has been selected to identify the interval of causal relationship between the two phenomena.

The TE in its turn shows basically the same trend in the set of discharges investigated. TE tends to increase slightly for very short time lags, reaches a constant levels and then decreases quite sharply for higher lag times (see Figure 8). This is a typical behaviour of dynamical systems; the triggering event has a significant influence for a specific window of opportunity, outside which it becomes quickly ineffective. Pellets seem to behave in a similar way. In a short time interval, they have the largest probability of triggering an ELM collapse. This probability then decays rapidly when pellet reach the plasma too far away from the completion of the natural cycle of the ELMs. On the other hand, if pellets arrive to close to the end of the natural ELM cycle, they are less effective in influencing their dynamics. The triggering efficiency, defined as the interval for successful triggering of the ELMs, can be calculated as the time point when the TE decays to 95% of its peak value excluding times shorter than 1 ms . In fact, this 95% has been chosen as a statistical "confidence interval"; in other words, performing many numerical tests, with pulses with shape and level of noise similar to the experimental values, it has been found that the transfer entropy curve broadens. This translates into the fact that 95% of TE maximum value typically provides the best

Table I. Characteristics of the pellets for the investigated discharges.

Pulse	#ELMs	#Pellets	Nominal Frequency [Hz]	Real Frequency [Hz]	Mass [N_A]	Speed [m/s]
84688	47	33	25	16.5	0.0299	80
84690	57	57	25	16.3	0.0299	80
84693	44	36	25	18.0	0.0332	80
82885	87	116	50	29.0	0.0349	176
82886	77	94	50	31.3	0.0349	170
82887	63	83	50	27.7	0.0349	200
82889	65	77	50	19.3	0.0349	174
84696	38	43	50	14.3	0.0332	80

estimate of the right time lag for signals of the shape typical of ELMs, almost always more reasonable than the maximum of TE. Moreover, the value of 95% is sufficiently conservative to assure that the effectiveness of the pellet triggering is not overestimated.

In the case of JRP, the evolution of several analysis measures with the lag time has been calculated: average of diagonal length, entropy of diagonal length, recurrence time, determinism. Events (=peaks) have been searched in the trends of these parameters with the lag time. Once an event is detected in the evolution of multiple parameters, the peak position is determined using the most distinctive peak. This peak defines the period of maximum correlation between the dynamics of the two systems and therefore it is assumed to identify an appropriate range over which the causal relation is effective. An example is shown in Figure 9.
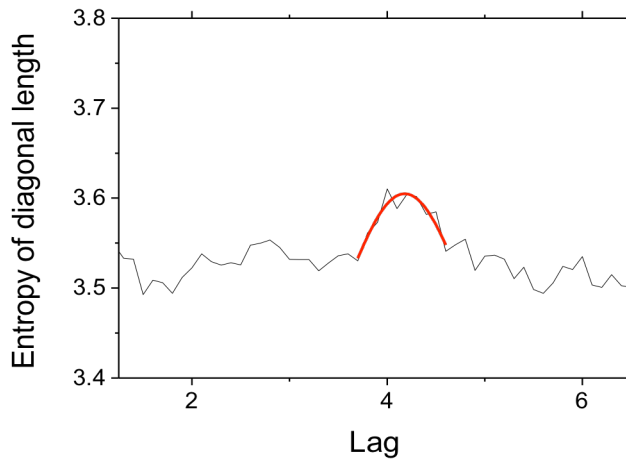

Figure 9. Discharge 82855. A peak is very evident in the entropy of diagonal length. The entropy of diagonal length has been fitted with a spline to identify the maximum (red curve)

In Table II, the lag times calculated with the three proposed techniques have been reported. The estimates are very similar and basically agree with each other within the error and uncertainties in the experimental data. The efficiency of the ELM triggering is also reported in the same Table II. This efficiency is calculated as the number of pellets triggering an ELM divided by the total number of pellets. A pellet is considered to have triggered the subsequent ELM if it has reached the plasma within the time lag identified by the corresponding criterion. For completeness the efficiency of the pellet triggering is reported also for the case of 2 ms lag time, traditionally used in JET.

The first interesting observation emerging from the proposed analysis is that the three indicators provide very similar results. The discrepancy is typically of the order of a fraction of a millisecond between the estimates of TE and JRP, which is certainly the limit of the accuracy which can be achieved given the measurements available. The maximum discrepancy is of 0.6 ms. The weakest estimate is typically the GC, which is known to be quite sensitive to noise and pulse shaping. Indeed it should be mentioned that the quality of the experimental signals is not very high, considering the complexity of the phenomenon, the

limited time resolution of the measurements and the level of added noise. Therefore, since the

Table II. Percentage of triggering for the lag times calculated with GC, TE, JRP and with the usually assumed of 2 ms. The percentages are calculated from the ratio of the number of ELMs triggered by pellets, divided by the total number of pellets reaching the plasma for each shot.

Pulse	Δt GC [ms]	GC % triggering	Δt TE [ms]	TE % triggering	Δt JRP [ms]	JRP % triggering	Δt=2 [ms]	2 ms % triggering
82885	1.5	6	1.5	6	1.5	6	2	7
82886	3.5	15	3.8	17	3.3	15	2	6
82887	3.6	19	4.1	23	4.2	24	2	11
82889	4.2	21	4.5	21	4.5	21	2	4
84688	1.8	9	1.3	3	1.8	9	2	9
84690	3.8	30	3.2	21	3.4	25	2	14
84693	3.1	25	3.5	28	3.2	25	2	17
84696	3.4	9	3.5	9	3.5	9	2	2

three approaches are numerically fully independent, the found agreement increases significantly the confidence in the obtained estimates. Moreover, the maximum discrepancy between the indicators can be treated as a confidence interval in the estimates. This is another important added value of the proposed approach, since using a fixed lag time of 2ms does not allow to provide any confidence interval in the results.

The other aspect to notice is that not all discharges show the same behaviour. Therefore assuming a single time interval of 2 ms, for calculating the number of ELMs triggered by pellets, is not completely adequate, since the lag times found with the three proposed methods range between 1.5 and 4.5 ms. The 2 ms interval previously assumed is a quite good estimate on average but should be particularised for each discharge. Indeed, assuming a fixed 2 ms interval, the actual triggering efficiency can be either overestimated or underestimated. This can lead to misleading interpretation of actions taken in the experiments, which can be wrongly considered to have the opposite effect on the triggering efficiency than the real one.

In any case, on average the choice of 2 ms lag time leads to an unnecessary underestimate of the triggering efficiency of the pellets, at least for the discharges considered in this paper.

7 Discussion and Conclusions

In this paper, three different statistical approaches to the assessment of the triggering efficiency of ELMs have been introduced. Two of them, Granger Causality and Transfer
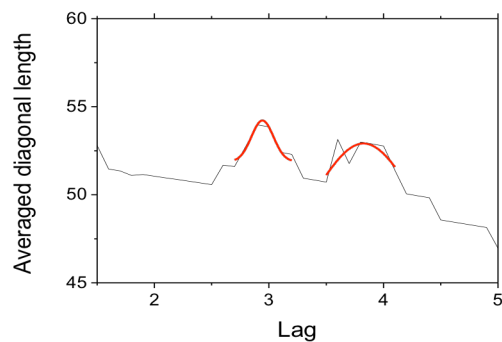

Figure 10 Average diagonal length for discharge 82854. The presence of two lag times is quite evident. The second peak corresponds to a specific interval of the discharge between 51 and 52 s (see Figure 11).

Entropy, implement a causality concept based on increased predictability. Transfer Entropy does not relay on any assumption about linearity of the underlying dynamics and therefore it is more general than the implemented version of Granger Causality. On the other hand, the two criteria are numerically completely independent. The third method exploits the properties of Joint Recurrence Plots and is based on the analyses of the recurrence properties of dynamical systems.

A series of numerical tests has shown the potential of the three techniques to determine the time interval over which a causal-effect relationship takes place. All three criteria have proved to possess excellent qualities of prediction and produce the expected results also for spiky signals of the type typical of ELMs.

The application of the three criteria to ELMs pellet pacing experiments on JET with the ILW gives very coherent and similar outputs, which can also help in quantifying the uncertainty in the estimates. The obtained results indicate that the traditional criterion use to estimate the efficiency of pellets underestimates on average the capability of this system to trigger ELMs. On the other hand, every discharge is a different case and must be studied independently. Indeed the appropriate lag time to calculate the number of ELMs triggered by

pellets ranges between1.5 and 4.5 ms. The proposed criteria therefore allows assessing the properties of pellets on a shot to shot basis, paving the way for a much better understanding and optimization of this important tool in the perspective of ITER. It is also worth mentioning that the proposed techniques, being based on the statistical relations between pellets and ELMs, are not influenced by changes in the base plasma parameters. Indeed the injection of pellets can induce increases in the plasma density at the edge, rendering even more difficult the interpretation of the results if a fixed lag time is used, since the change in the ELM frequency can be due to those variations of the average density and not to the pellet pacing capability. The two effects are difficult to disentangle if a fixed lag time is used as the criterion to evaluate the pellet pacing efficiency.

The proposed techniques seem to have even a higher time resolution, rendering them capable also of detecting changes during a single shot. Indeed there is no particular physical reason for the lag time to remain exactly constant over the entire discharge. JRPs have a particularly good time resolution as can be seen from the example reported in Figure 10 for shot number 82854. For this discharges, the JRP criterion identifies to different lag times: a first one around 2.9 ms and a second one at about 3.8 ms. The GC also provides two estimates: at 2.7 and 3.8 ms. These two different estimates correspond to two differ phases of the discharge, as can be seen in the trend of the D_α reported in Figure 11. If the interval between 51 and 52 s is removed from the analysis only the lag time around 2.7 ms remains. On the contrary, if only the interval between 51 and 52 ms is considered, the lag time
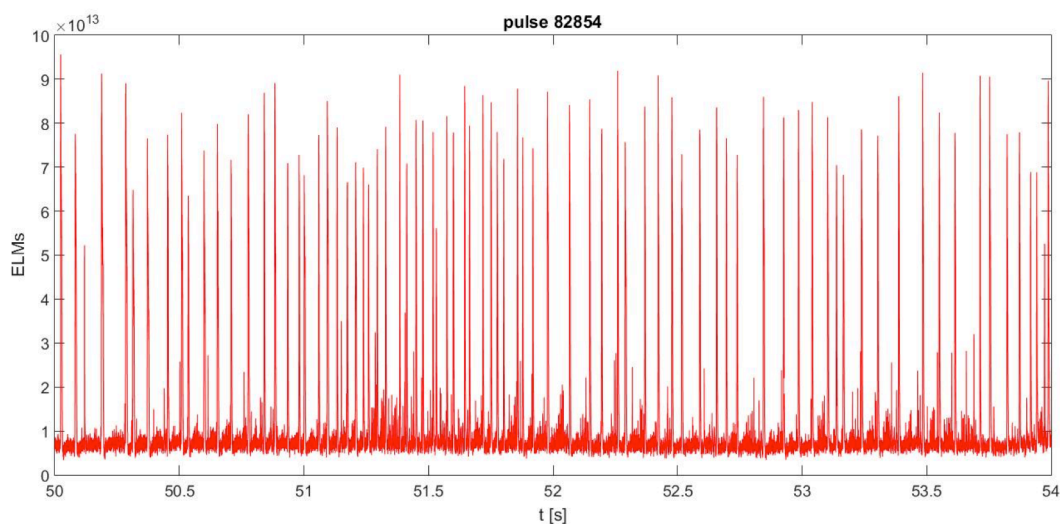

Figure 11 Dα for shot number 82854.A different phase of increased frequency appears around about 51 and 52 ms.

remaining is 3.8 ms. Therefore, the increase in the ELM frequency in the period between 51

and 52 s seems really linked to an increase in the efficiency of the pellet pacing. On the other hand, the statistics in these discharges is not very high so this result must be considered as preliminary. In any case, it can be stated that, even the three criteria are statistical in nature and require enough data at steady state, if different but sufficiently long stationary intervals are present during a single discharge, they can provide specific information on these intervals. Such a capability provides the opportunity to particularise the analysis and even to perform different experiments in the same discharge.

With regard to future developments, first it should be mentioned that the application of these tools to Tokamak physics seems quite promising. Indeed, traditionally in many cases the causal relationship between time series is determined by simple visual inspection of the signals and the determination of time proximity of events. In some applications, it is also necessary to make recourse to not well-founded simplistic hypotheses. These visual inspection exercises are quite prone to errors and misinterpretations. Therefore, the proposed techniques, based on sound statistical and dynamical tools, are expected to have significant potential. They could indeed be used to consolidate preliminary investigations, to critically test working hypotheses and to address completely new issues. Three potential very promising fields are the investigation of instabilities, studies of plasma dynamics and control of impurities. Among various instabilities, the assessment of the disruption causes seems particularly relevant. The present investigations of this very important aspect have been limited so far by some weaknesses that the proposed methods could help to alleviate. First, the choice of the most significant signals for disruption prediction on JET has been based on empirical considerations without solid statistical basis. In this perspective, the three methods introduced in this paper could be usefully deployed to identify the most appropriate signals to include in disruption predictors for the optimization of their performance [12-18]. They could also play a role on the assessment of the quality of various mitigation strategies. With regard to disruption avoidance, the contribution of the proposed techniques could be even more fundamental, since the investigation of the best strategies to reduce the percentage of disruptions is even less mature than prediction for mitigation. With regard to plasma dynamics, an interesting subject is certainly the L-H transition, for which various models exist but no accepted dynamical theory is available. The tools presented in this paper could be deployed to provide a statistical sound analysis of the most likely quantities to be the control parameters for this transition [19-20]. Another aspect of Tokamak control, which presents serious challenges, is impurity control [21]. This issue has become particularly relevant since the installation of the new ILW. Given the difficulties in the impurity dynamics, their link

with sawteeth and ELMs and the quality of the measurements, sound statistical criteria to assess the efficiency of the various control strategies are expected to be quite beneficial. Another important potential application is the qualification of the magnetic equilibria, which are essential to control the configurations and to maximise performance. On the other hand, statistical methods have not been applied much so far to detect problems ion the reconstructions and to determine the relations between possible causes [22,23]

References

[1] J. Wesson, *"Tokamaks"*. Oxford : Clarendon Press Oxford, 2004. Third edition.

[2] Wesson, J.A., et al., Nuclear Fusion, 1989. **29**(4): p. 641.

[3]Barbara Cannas, Alessandra Fanni, Andrea Murari, Fabio Pisano *"Nonlinear dynamic analysis of D_α signals for type I Edge Localized Modes characterization on JET with a carbon wall"* submitted to Plasma Physics and Controlled Fusion

[4] A. Murari et al *"Upgrades of Diagnostic Techniques and Technologies for JET next D-T Campaigns"* submitted to Transactions on Nuclear Science

[5] D.Frigione et al *Journal of Nuclear Materials ,***2015***, 463*, 714 - 717 [1]N. Wiener, in Modern Mathematics for Engineers, editedby E. Beckenbach (McGraw-Hill, New York, 1956).

[6] L.Garzotti et al *Plasma Physics (Proc. 37th EPS Conf. Dublin, 2010), European Physical Society,* **2010***, 34A*, P2.131

[7]N. Wiener, in Modern Mathematics for Engineers, edited by E. Beckenbach (McGraw-Hill, New York, 1956).

[8] C. Granger, Econometrica 37, 424 (1969).

[9] T. Schreiber, Phys. Rev. Lett. 85, 461 (2000).

[10] N.Marwan wt al Physics Reports 438 (2007) 237 – 329)

[11] Kenneth P. Burnham, David R. Anderson (2002), *Model Selection and Multi-Model Inference: A Practical Information-Theoretic Approach*. Springer. (2nd ed)

[12] G. A. Rattá, et al. Nuclear Fusion. 50 (2010) 025005 (10pp).

[13] B. Cannas et al Nucl. Fusion 53 093023 doi:10.1088/0029-5515/53/9/093023.

[14] A.Murari et al,Nucl. Fusion **53** (2013) 033006 (9pp)

[15] J. Vega, et al Nuclear Fusion. 49 (2009) 085023 (11pp)

[16] A. Murari et al 2013 *Nucl. Fusion***53** 043001 doi:10.1088/0029-5515/53/4/043001

[17] A.Murari, et al Nucl. Fusion**49**(2009) 055028 (11pp)

[18] Hender, T.C., et al., *Chapter 3: MHD stability, operational limits and disruptions.* Nuclear Fusion, 2007. **47**(6): p. S128-S202.

[19] A. Murari et al 2012 *Nucl. Fusion* **52** 063016 doi:10.1088/0029-5515/52/6/063016

[20] A. Murari et al (2013) *Nucl. Fusion* **53** 043001 doi:10.1088/0029-5515/53/4/043001

[21] M.E.Puiatti et al Plasma Physics and Controlled Fusion, **44** (9), pp. 1863-1878 (2002).

[22] A.Murari et al Nucl. Fusion **51** (2011) 053012 (18pp) doi:10.1088/0029-5515/51/5/053012

[23] M.Gelfusa et al Review of Scientific Instruments **84**, 103508 (2013) and may be found at doi: 10.1063/1.4824200